

#### **Experimental Research Article**

# Correlation between knee pain and quadriceps condition in osteoarthritis rats treated with cog polydioxanone filaments

Myeounghoon Cha<sup>1,2</sup>, Guanghai Nan<sup>1,3</sup>, Nari Kang<sup>1</sup>, Sun Joon Bai<sup>4</sup>, Ryo Ikeda<sup>5,6</sup>, Bae Hwan Lee<sup>1,3,7</sup>, and Jun Ho Jang<sup>8</sup>

<sup>1</sup>Department of Physiology, Yonsei University College of Medicine, Seoul, Korea, <sup>2</sup>Department of Physiology, College of Medicine. Soonchunhvang University, Cheonan, Korea, <sup>3</sup>Brain Korea 21 FOUR Project for Medical Science, Yonsei University College of Medicine, Seoul, Korea, <sup>4</sup>Department of Anesthesiology and Pain Medicine, Anesthesia and Pain Research Institute, Yonsei University College of Medicine, Seoul, Korea, <sup>5</sup>Department of Orthopaedics, Jikei University School of Medicine, Tokyo, Japan, <sup>6</sup>Department of Orthopaedic Surgery, Tokyu Hospital, Tokyo, Japan, <sup>7</sup>Brain Research Institute, Yonsei University College of Medicine, Seoul, Korea, <sup>8</sup>R&D Center, OV MEDI Co., Ltd., Gunpo, Korea

Background: Weakness in the quadriceps muscle significantly contributes to the development and progression of knee osteoarthritis (OA), characterized by pain and impaired function. This study aimed to assess structural and functional recovery in the quadriceps and its association with knee OA pain following treatment with the Muscle Enhancement and Support Therapy (MEST) device. MEST involves inserting cog polydioxanone filaments directly into muscle tissue to help alleviate OA pain.

Methods: Knee OA was induced in Sprague-Dawley rats using monoiodoacetate injections, followed by MEST or a sham treatment. Five weeks post-MEST treatment, quadriceps recovery was evaluated by measuring entire muscle volume, hindlimb torque, tissue morphology, and key structural and functional biomarkers. Pain was assessed through paw withdrawal thresholds and weight-bearing distribution. Correlations between muscle measurements and pain levels were then analyzed.

Results: MEST treatment resulted in significant increases in quadriceps volume, enhanced hindlimb torque, and elevated expression of α-actin, myosin, and the mitochondrial marker cytochrome c oxidase subunit 4, along with reductions in OA pain. These enhancements in muscle condition were closely associated with pain relief in OA.

Conclusions: This study shows that MEST improves the quadriceps condition, including muscle volume, structure, function, and energy metabolism, and relieves knee OA pain, which are closely linked. These findings may suggest that promoting quadriceps recovery through MEST could be a promising approach for managing OA-related pain.

Keywords: Joint; Knee; Muscle; Osteoarthritis; Pain; Polydioxanone; Quadriceps.

Received November 11, 2024; Revised January 26, 2025; Accepted January 27, 2025

Handling Editor: Woong Mo Kim Correspondence: Bae Hwan Lee

Department of Physiology, Yonsei University College of Medicine, 50-1, Yonsei-ro, Seodaemun-gu, Seoul 03722, Korea Tel: +82-2-2228-1711, Fax: +82-2-393-0203, E-mail: bhlee@yuhs.ac

Jun Ho Jang

R&D Center, OV MEDI Co., Ltd., 2F, 117, Gongdan-ro, Gunpo 15847, Korea Tel: +82-70-4916-6116, Fax: +82-2-838-0569, E-mail: junho@ovmedi.com

This is an Open Access article distributed under the terms of the Creative Commons Attribution Non-Commercial License (https://creativecommons.org/ licenses/by-nc/4.0), which permits unrestricted non-commercial use, distribution, and reproduction in any medium, provided the original work is properly cited.



# INTRODUCTION

Osteoarthritis (OA) is a chronic degenerative joint disease, primarily characterized by the progressive deterioration of articular cartilage and subsequent bone remodeling, leading to pain and functional impairment. It is the most common form of arthritis, affecting millions of individuals worldwide, with the knee joint being one of the most frequently involved sites [1–3]. Current treatment approaches, including non-pharmacological, pharmacological, and surgical interventions, primarily focus on symptom management, with a particular emphasis on pain relief. Despite advances in care, there remains no definitive disease-modifying therapy for OA [1–5].

Beyond the pathological changes within the joint, quadriceps weakness is a prevalent and significant condition in patients with knee OA, contributing to both the progression and severity of the disease [6–8]. This muscle weakness can arise from several factors, including disuse atrophy resulting from decreased activity [9], arthrogenic muscle inhibition, which is a neural response that limits the full activation of muscles around an injured joint [10], and decreased physical function secondary to pain [11]. Periarticular muscle weakness compromises joint stability and protection [12–18], leading to altered biomechanics and abnormal joint loading [17,19], which perpetuates cartilage degradation and further disability. This process contributes to the exacerbation of OA pain and functional limitations [20].

Previous animal and clinical studies have shown promising results for the Muscle Enhancement and Support Therapy (MEST) device, which was recently approved by the Korean Ministry of Food and Drug Safety. The MEST device is designed to implant cog polydioxanone filaments into the quadriceps to relieve knee OA pain [21-24]. One of the proposed mechanisms for the analgesic effect of MEST involves the restoration of atrophied and weakened quadriceps, thus potentially enhancing joint stability and biomechanics, while simultaneously reducing articular nociceptor sensitization [21,22,24]. In these studies, muscle recovery from atrophy was observed alongside pain relief. While this mechanism is plausible, specific changes of the quadriceps condition such as total muscle volume, structural components, function, and energy metabolism, as well as their direct correlation with OA pain relief, have yet to be firmly determined.

This study aimed to evaluate the structural and functional changes in the quadriceps (primary outcome) and pain relief (secondary outcome) and to analyze their correlation following MEST treatment in knee OA rats.

Five weeks post-MEST treatment, the quadriceps condition was evaluated through assessments of the whole quadriceps volume, hindlimb torque, and structural and functional biomarkers including  $\alpha$ -actin, myosin, and cytochrome c oxidase 4 (COX4). The correlations between these individual measurements and pain-related behaviors were then evaluated.

# MATERIALS AND METHODS

#### 1. Animals

The experimental procedures were approved by the Institutional Animal Care and Use Committee of Yonsei University Health System (#2021-0285), ensuring adherence to all pertinent regulations and guidelines. Conforming to the Animal Research: Reporting of *In Vivo* Experiments (ARRIVE) guidelines, meticulous reporting of the experiments was ensured. Male Sprague-Dawley rats (Orient Bio), aged 6–7 weeks at the commencement of the experiments, were housed in groups of three to four. They had unrestricted access to food and water within a 12-hour light/dark cycle throughout the study period.

#### 2. OA induction

The authors utilized the monoiodoacetate (MIA) model of OA, which is recognized as a highly reliable and frequently employed chemical model. This model is particularly suitable for investigating the efficacy of novel treatments targeting OA-related pain [25]. Rats underwent intra-articular knee injections of MIA (Sigma Aldrich) in the left hindlimb while briefly anesthetized with isoflurane. A 1 mg dose was delivered initially, followed by a second injection of 3 mg two weeks later, both in 30  $\mu L$  of saline solution. This protocol was selected based on a previous study where a single MIA injection (1 mg) did not produce significant impairments in certain pain behaviors after two weeks [21]. Consequently, a second injection was added in later studies [22,24], including the present one.

#### 3. MEST treatment

The detailed methodology for the MEST device (MEST-B2375; OV MEDI) has been described previously [21]. The device includes a 23-gauge needle, a biodegradable PDO filament (0.3 mm outer diameter) featuring bidirectional cogs, and a protective catheter that shields the



cogs during the insertion process. After inducing brief anesthesia with pentobarbital (50 mg/kg, intraperitoneal [i.p.]), the thigh of the left hindlimb was shaved and prepared. The filament-loaded MEST needle was inserted approximately at one-third of the length of the quadriceps from the knee joint, then advanced toward the distal femur. Once positioned, the needle and catheter were retracted in sequence, leaving the cog filament securely embedded in the quadriceps muscle. Five filaments were evenly distributed across the quadriceps. Any exposed portions of the filaments were trimmed, and the incision was sutured. For the sham group, the same procedure was followed, but an empty needle was used, without the PDO filament insertion.

#### 4. Experimental design

The timeline and flowchart of the experimental design, including detailed sample sizes, are provided in **Fig.** 1. A total of 72 animals were randomly allocated to the following 6 groups (n = 12 per group) using a manual simple randomization technique, where group assignments were determined by drawing lots: (i) naïve group: untreated; (ii) MIA group: received 1st and 2nd MIA injections at weeks 0 and 2, respectively; (iii) MIA + MEST: received MIA injections followed by MEST treatment at week 3; (iv) MIA + sham: received MIA injections followed by sham treatment at week 3; (vi) naïve + sham: received MEST treatment at week 3; (vi) naïve + sham: received sham treatment at week 3. Double blinding was maintained throughout the experiment to prevent bias.

This included blinded experimental procedures, where researchers administering treatments or performing measurements were unaware of group assignments, and blinded data analysis, where individuals conducting tissue analysis and statistical evaluations were also blinded to the group allocations. Data acquisition and analysis were performed by separate experimenters to further ensure objectivity. Sample sizes were determined based on prior studies that used the same animal model and MEST treatment for pain relief [21,22,24]. Although statistical power or effect sizes were not calculated beforehand, the observed significant differences in key outcomes across previous and current experiments indicate that the sample sizes were adequate to detect meaningful effects. Future studies will benefit from pre-calculated power analyses to ensure rigorous validation.

All animals participated in behavioral experiments conducted at weeks 0, 3, and 8. Following final behavioral tests, magnetic resonance imaging (MRI) acquisition was performed (n = 10–12 animals/group) at week 8. Subsequently, animals were evenly divided into two groups at week 8: one for hindlimb torque experiments (n = 5–6 animals/group) and the other for immunohistochemistry staining (n = 6 animals/group). For immunohistochemistry analysis, 8–9 slides per group were randomly selected from each cohort, with at least one slide obtained from each animal. Additional images were occasionally included to ensure a sufficient number of high-quality, analyzable images per group. The total number of images used for cell count analysis was 17–18 per group, encompassing slides where  $\alpha$ -actin and myosin were double-

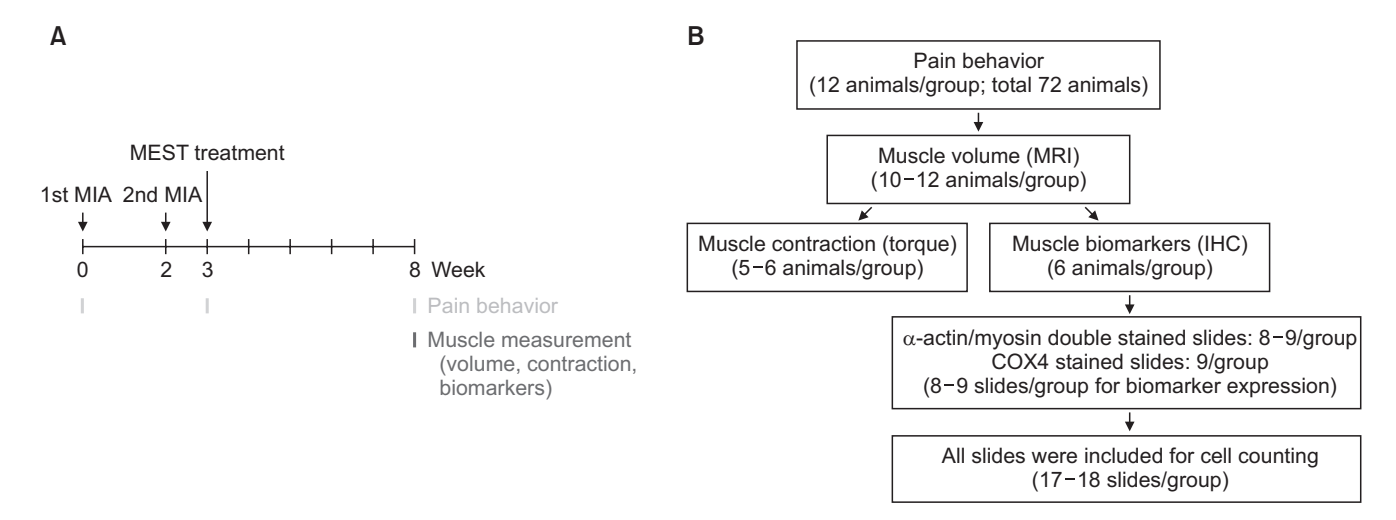


Fig. 1. Timeline and flowchart of the experimental design. (A) Timeline of the experimental design. (B) Flowchart illustrating the experimental procedure and sample sizes. MEST: Muscle Enhancement and Support Therapy, MIA: monoiodoacetate, MRI: magnetic resonance imaging, COX4: cytochrome c oxidase 4, IHC: immunohistochemistry.



stained (8–9 slides/group) and COX4 was independently stained (9 slides/group). Detailed N numbers for individual groups are indicated in the figure legends. Animals not included in the data analysis were used to set the experimental conditions.

#### 5. von Frey test

Mechanical pressure was applied to the plantar surface of the left hind paw using an electronic von Frey apparatus (UGO Basile) to assess the paw withdrawal threshold (PWT). Rats were placed in individual enclosures on a perforated platform and allowed to acclimate to the testing environment for 30 minutes prior to testing. The probe was applied perpendicularly to the paw, and the force required to elicit a withdrawal response was automatically recorded. The cut-off value was set at 300 g to prevent tissue damage. Each rat underwent five trials with a 3-minute interval between trials, and the PWT values were averaged to determine the final measurement.

#### 6. Weight-bearing test

The rats were placed inside a plexiglass chamber, with each hind paw positioned on separate force plates of an incapacitance tester (Linton Instrumentation). The force applied by each hindlimb was recorded over a 5-second period, and the average force was used to calculate the weight-bearing ratio (WBR), which reflects the load borne by the left hindlimb compared to the right.

#### 7. MRI acquisition

MRI scans of the left quadriceps were conducted under isoflurane anesthesia (5% for induction and 1.5%-2% for maintenance) using a 9.4-T horizontal Biospec small bore scanner (Bruker BioSpin). The system was equipped with an 86 mm volume coil for radio frequency transmission and a four-channel array coil for signal reception. Following tuning and shimming, initial T2 spin echo sequence images were acquired to ensure accurate positioning, followed by T1-weighted (T1W) images at the corresponding locations. High-resolution anatomical images were captured using a rapid acquisition with relaxation enhancement (RARE) protocol, with the following parameters: effective echo time (TE) = 22 ms, repetition time (TR) = 2,300 ms, matrix size =  $512 \times 256$ , and RARE factor = 4. Additionally, 25 slices of T1W images were obtained using the RARE protocol with a shortened TR and the following settings: RARE factor = 4, TE/TR = 18.61/800 ms, matrix size =  $192 \times 192$ , and slice thickness = 1 mm. Throughout the procedure, respiration rates of the animals were closely monitored. The hindlimb was segmented on axial slices, and the mean area of the quadriceps was measured. Image analysis was performed using 3D Slicer software (version 5.2.1), and the analyzed 25 slices encompassed the entire MEST-treated quadriceps region, excluding the upper portions due to interference from fat and intestinal organs.

# 8. Hindlimb torque evaluation

Maximum hindlimb torque generated by quadriceps contraction was assessed under urethane anesthesia (0.5 g/kg, i.p.). For precise measurements, the left knee joint was stabilized in an axial position, and a digital torque meter (HP-100; HIOS) was employed. Quadriceps contraction was induced by electrically stimulating the femoral nerve using needle electrodes, with pulse durations set to 10 ms and amplitudes of 1, 2, or 3 mA. Proper electrode placement was confirmed by observing a series of isometric twitches and isolated knee extensions.

#### 9. Immunohistochemistry

The left quadriceps were harvested and cryosectioned at a thickness of 20 µm. These sections were then incubated overnight with primary antibodies (Abcam) against  $\alpha$ -actin (1:100; ab184705; RRID:AB\_3472024), myosin (1:1,000; ab37484; RRID:AB\_2921304), or COX4 (1:600; ab16056; RRID:AB\_443304). This was followed by incubation with secondary antibodies (Jackson ImmunoResearch) Alexa Fluor 488 (1:1,000; #715-166-151; RRID:AB\_2341099) or Cy<sup>™</sup>3 (1:1,000; #711-545-152; RRID: AB 2922842). Cell nuclei were counterstained with DAPI. Immunofluorescent images were captured using a confocal microscope (LSM700; Zeiss). Analysis was conducted in a randomly selected region of interest (ROI) from the tissue slide. Biomarker expression levels were quantified based on intensity values, which were divided by the number of cells in the ROI to estimate the intensity per cell. Cells were included in the cell count if the ROI covered approximately 70% or more of the cell area.

#### 10. Data analysis

To assess group differences at a single time point, a one-way analysis of variance (ANOVA) was applied, with Tukey's *post-hoc* test used for four groups and an unpaired *t*-test for comparisons between two groups.



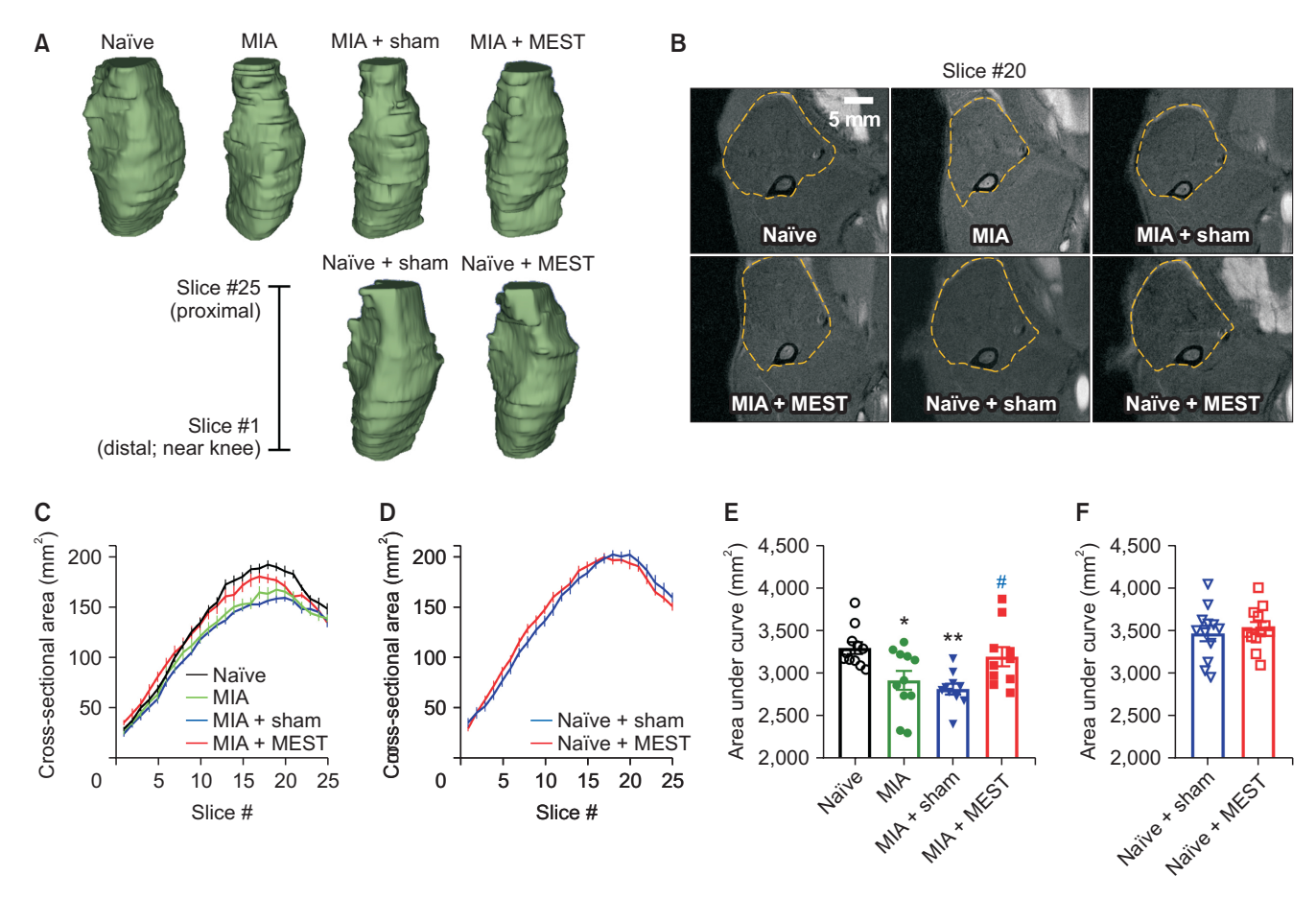


**Fig. 2.** MEST restores MIA-induced muscle volume reduction. (A) Representative 3D reconstructions of the quadriceps based on 25 MRI slice images. (B) Cross-sectional images (slice #20) corresponding to panel (A), with yellow dotted lines indicating the quadriceps area and thick black lines outlining the femur bone. (C, D) Cross-sectional area measurements. (E, F) AUC calculated from the measurements in panel (C, D). Naïve: N = 11, MIA: N = 11, MIA + Sham: N = 10, MIA + MEST: N = 10, Naïve + Sham: N = 12, Naïve + MEST: N = 12. \*P < 0.05, \*\*P < 0.01 vs. Naïve. \*P < 0.05 vs. MIA + Sham. Data are presented as mean  $\pm$  standard error of the mean. Statistical analyses: one-way ANOVA followed by Tukey's multiple comparison test (E) or unpaired t-test (F). MEST: Muscle Enhancement and Support Therapy, MIA: monoiodoacetate, MRI: magnetic resonance imaging, AUC: area under the curve, ANOVA: analysis of variance.

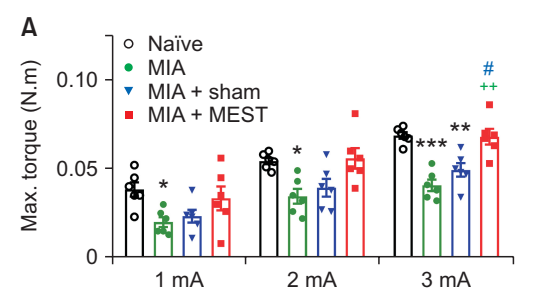
For analysis involving repeated measurements across multiple time points or under different experimental conditions at a given time, a two-way repeated measures ANOVA was conducted, followed by Tukey's test for four groups or Sidak's test when comparing two groups. Pearson's correlation coefficients were used to evaluate the relationships between muscle conditions and pain behaviors. Data are presented as mean  $\pm$  standard error of the mean. Statistical significance was set at P < 0.05. All statistical analyses were performed using Prism 7.0 software (GraphPad Software; RRID:SCR 002798).

# **RESULTS**

# 1. MEST-induced restoration of muscle volume

The authors examined whether the MEST treatment affected the entire quadriceps volume using MRI scans at week 8 (**Fig. 2**). Representative reconstructed 3D (**Fig. 2A**) and cross-sectional (**Fig. 2B**) images of the quadriceps illustrate a decrease in muscle volume due to MIA injections and restoration with MEST treatment. Further analysis of cross-sectional areas reveals that the area under the curve (AUC) of the quadriceps in the MIA group is smaller than that of the naïve quadriceps (**Fig. 2C, E**). The MIA + MEST group exhibited an increased AUC compared to the MIA + sham group, demonstrating the





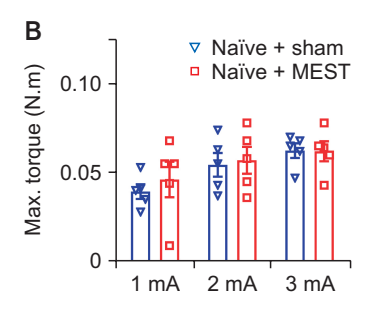


**Fig. 3.** MEST restores MIA-induced reduction in hindlimb torque. (A, B) The maximal torque force of the hindlimb elicited by electrical stimulation of quadriceps. Electrical stimulation with 10-ms pulse durations at amplitudes of 1, 2, or 3 mA was delivered to elicit quadriceps contraction and hindlimb torque. Naïve: N = 6, MIA: N = 6, MIA + Sham: N = 6, MIA + MEST: N = 6, Naïve + Sham: N = 6, Naïve + MEST: N = 5. \*P < 0.05, \*\*P < 0.01, \*\*\*P < 0.001 vs. Naïve. \*P < 0.01 vs. MIA. \*P < 0.05 vs. MIA + Sham. Data are presented as mean  $\pm$  standard error of the mean. Statistical analyses: two-way repeated measures ANOVA followed by Tukey's (A) or Sidak's (B) multiple comparison test. MEST: Muscle Enhancement and Support Therapy, MIA: monoiodoacetate.

restoration of quadriceps volume due to MEST treatment (**Fig. 2C, E**). However, neither MEST nor sham treatment in the naïve group resulted in significant changes in AUC (**Fig. 2D, F**).

#### 2. MEST-induced restoration of muscle function

At week 8, quadriceps strength was evaluated by measuring hindlimb torque (Fig. 3). Both the MIA and MIA + sham groups exhibited a marked reduction in maximum torque force generated by electrical stimulation at varying intensities (1, 2, or 3 mA), compared to the naïve group (Fig. 3A). This reduction was significant across all stimulation levels for the MIA group, while the MIA + sham group only showed a significant decline at 3 mA. In contrast, the MIA + MEST group showed an improved torque force at 3 mA when compared to both the MIA and MIA + sham groups (Fig. 3A), indicating that MEST treatment successfully restored quadriceps strength in the MIA group. However, no significant differences were found at the 1 and 2 mA stimulation levels. Additionally, the comparison between naïve animals treated with either the sham procedure or MEST revealed no significant difference in maximum torque force at any of the stimulation intensities (Fig. 3B).

# MEST-induced restoration of muscle density and biomarkers

At week 8, quadriceps muscle condition was evaluated by examining both cell density and the expression levels of key biomarkers, including  $\alpha$ -actin, myosin, and COX4 within the ROI (**Fig. 4**). The number of muscle cells was notably higher in the MIA and MIA + sham groups

compared to the naïve group (Fig. 4B). Treatment with MEST led to a significant reduction in cell numbers in MIA animals, compared to both the MIA and MIA + sham groups (Fig. 4B), suggesting effective reversal of muscle atrophy. Additionally,  $\alpha$ -actin expression per cell was lower in the MIA and MIA + sham groups relative to naïve controls (Fig. 4D). However, this reduction was significantly restored in the MIA + MEST group, as compared to both the MIA and MIA + sham groups (Fig. 4D). Similar trends were observed for myosin and COX4 expression: both were reduced in the MIA and MIA + sham groups compared to naïve animals, but the MIA + MEST group showed a significant recovery in these biomarker levels (Fig. 4F, H). In naïve animals, neither MEST nor sham treatments had any notable effect on cell numbers or the expression of  $\alpha$ -actin, myosin, or COX4 (**Fig. 4C, E, G, I**).

#### 4. MEST-induced pain relief

The effects of MEST on MIA-induced pain behaviors were evaluated (**Fig. 5**). In naïve animals, PWT and WBR remained stable throughout the duration of the study. In contrast, MIA injections caused a significant decrease in both PWT and WBR by week 3, indicating the onset of pain hypersensitivity compared to naïve controls. This heightened sensitivity persisted through to week 8. Remarkably, animals treated with MEST at week 3 showed a significant recovery in both PWT and WBR by week 8, when compared to both the MIA and MIA + sham groups. In naïve animals, neither MEST nor sham treatment had any effect on PWT or WBR.



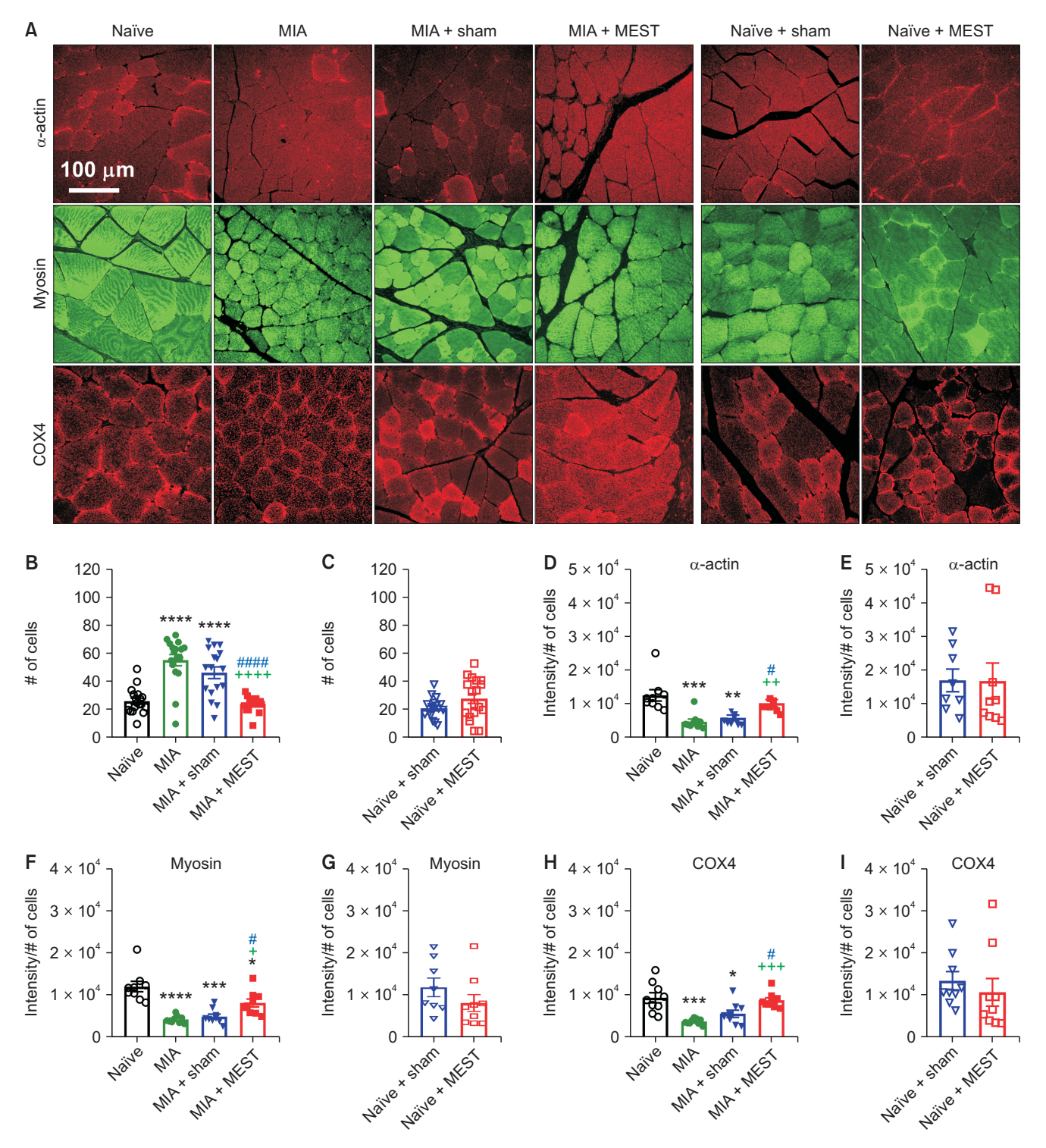


**Fig. 4.** MEST restores MIA-induced increase in muscle cell number and reduction in biomarker expression in the ROI. (A) Representative images of immunostaining. Scale bar, 100 μm. (B, C) Number of cells. Slide numbers used for analysis are as follows: Naïve: N = 18, MIA: N = 17, MIA + Sham: N = 17, MIA + MEST: N = 18, Naïve + Sham: N = 17, Naïve + MEST: N = 18. (D–I) Immunohistochemical analysis of muscle biomarkers. The expression intensity per cell of α-actin (D, E), myosin (F, G), and COX4 (H, I). Slide numbers used for analysis are as follows: For α-actin and myosin, N = 9 for all groups except Naïve + Sham, where N = 8. For COX4, N = 9 per group. \*P < 0.05, \*\*P < 0.01, \*\*\*P < 0.001, \*\*\*\*P < 0.001 vs. Naïve. \*P < 0.05, \*\*P < 0.001 vs. MIA. \*P < 0.001 vs. MIA + Sham. Data are presented as mean ± standard error of the mean. Statistical analyses: one-way ANOVA followed by Tukey's multiple comparison test (B, D, F, H) or unpaired *t*-test (C, E, G, I). MEST: Muscle Enhancement and Support Therapy, MIA: monoiodoacetate, ROI: region of interest, COX4: cytochrome c oxidase 4, ANOVA: analysis of variance.



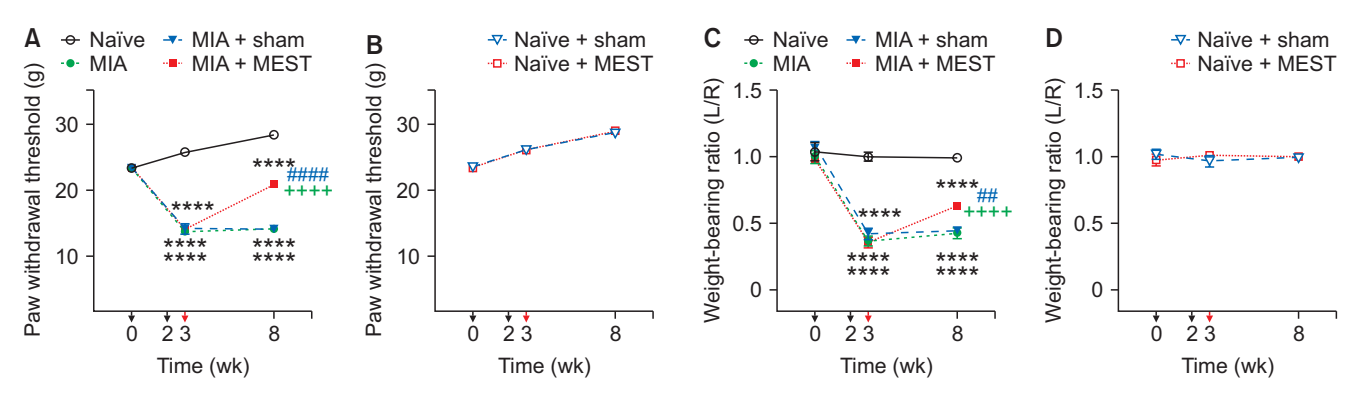


**Fig. 5.** MEST relieves MIA-induced pain. (A, B) PWT to von Frey filament. (C, D) WBR of the left over right hindlimb. Black arrowheads indicate MIA injections and red arrowhead indicates MEST treatment. N = 12 per group. \*\*\*\*P < 0.0001 V s. Naïve. \*\*\*\*P < 0.0001 V s. MIA. \*\*\*P < 0.001 V s. MIA + Sham. Data are presented as mean  $\pm$  standard error of the mean. Statistical analyses: two-way repeated measures ANOVA followed by Tukey's (A, C) or Sidak's (B, D) multiple comparison test. MEST: Muscle Enhancement and Support Therapy, MIA: monoiodoacetate, PWT: paw withdrawal threshold, WBR: weight-bearing ratio, ANOVA: analysis of variance.

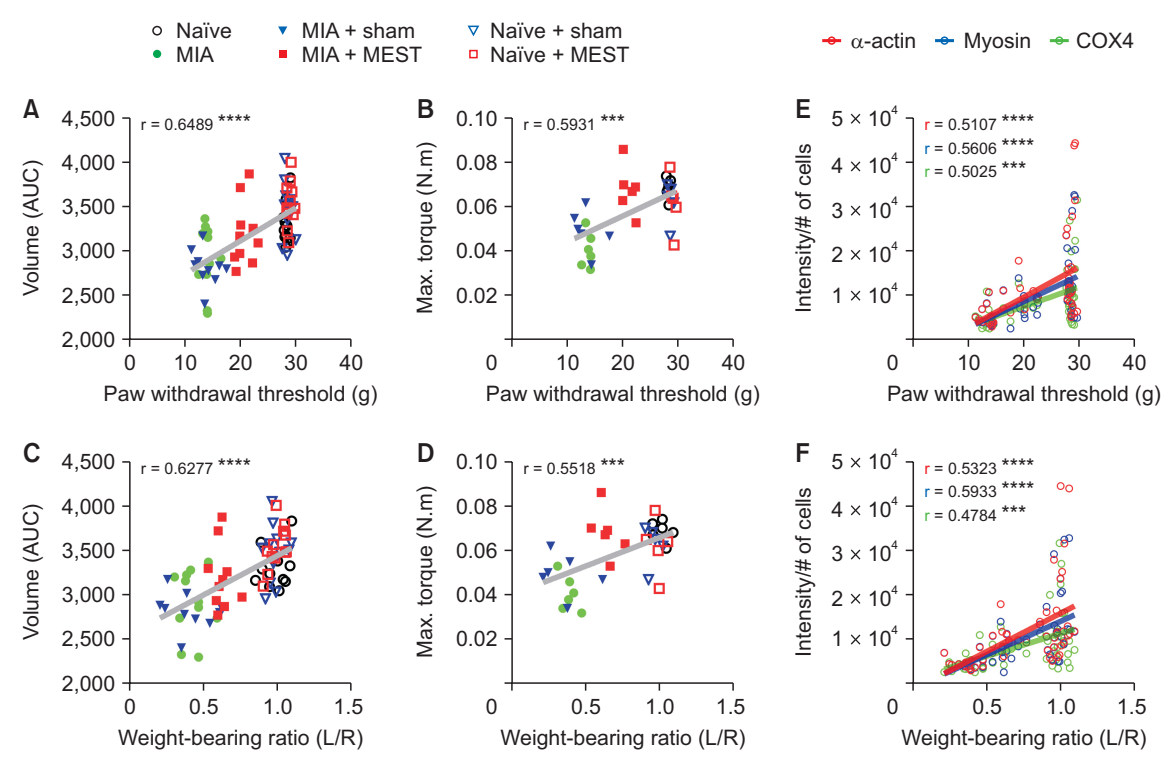


**Fig. 6.** MEST-induced muscle recovery correlates with pain relief. (A–D) Correlation analysis comparing muscle volume and maximum hindlimb torque elicited by 3 mA electrical stimulation with PWT (A, B) and WBR (C, D). (E, F) Correlation analysis relating the expression intensity, divided by cell numbers, of α-actin, myosin, and COX4 to PWT (E) and WBR (F). N numbers are the same as indicated in Figs. 2, 3, and 4. \*\*\*P < 0.001, \*\*\*\*P < 0.0001. Statistical analyses: Pearson's correlation coefficients test. MEST: Muscle Enhancement and Support Therapy, MIA: monoiodoacetate, PWT: paw withdrawal threshold, WBR: weight-bearing ratio, COX4: cytochrome c oxidase 4.

# Correlation between quadriceps condition and pain behaviors

At week 8, the correlation between quadriceps condi-

tion, assessed by muscle volume, hindlimb torque, and biomarker expression, and pain behaviors was evaluated (**Fig. 6**). Quadriceps volume assessed by AUC exhibited significant correlations with both PWT (r = 0.6489, P <



0.001, 95% confidence interval [CI]: 0.4827 to 0.7700; **Fig. 6A)** and WBR (r = 0.6277, P < 0.001, 95% CI: 0.4548 to 0.7550; Fig. 6C). Similarly, maximum torque of the hindlimb elicited by 3 mA stimulation of quadriceps correlated with both PWT (r = 0.5931, P < 0.001, 95% CI: 0.3188 to 0.7757; **Fig. 6B**) and WBR (r = 0.5518, P < 0.001, 95% CI: 0.2627 to 0.7500; Fig. 6D). The expression intensity, divided by cell numbers, of  $\alpha$ -actin (r = 0.5107, P < 0.001, 95% CI: 0.2790 to 0.6863), myosin (r = 0.5606, P < 0.0010.001, 95% CI: 0.3422 to 0.7216), and COX4 (r = 0.5025, P < 0.001, 95% CI: 0.2712 to 0.6789) showed significant correlations with PWT (Fig. 6E), as did their correlations with WBR ( $\alpha$ -actin: r = 0.5323, P < 0.001, 95% CI: 0.3061 to 0.7017; myosin: r = 0.5933, P < 0.001, 95% CI: 0.3847 to 0.7442; COX4: r = 0.4784, P < 0.001, 95% CI: 0.2415 to 0.6614) (Fig. 6F).

# DISCUSSION

The findings of this study demonstrate that MEST not only effectively alleviates knee OA pain but also promotes recovery in the atrophied and weakened quadriceps muscles. This is evident from the observed increases in whole muscle volume, improved contractile function, and the restoration of key biomarkers associated with muscle structure, function, and energy metabolism. The strong correlation between enhanced muscle condition and reduced knee OA pain suggests an association between MEST-induced improvements in the quadriceps' structural and functional state and the observed alleviation of OA-associated pain.

Previous studies have shown that MEST reverses quadriceps weakness and atrophy in MIA-induced OA models [20,23]. However, these studies assessed the reversal of muscle atrophy and reduced muscle weight through the weight ratio of a 3-mm thick slice of quadriceps tissue [24] or a portion of the quadriceps (rectus femoris muscle) [21] relative to body weight, supported by data from crosssectional tissue sections [21,24]. Furthermore, restoration of quadriceps contractile function was evaluated only in the early stages to trace the recovery process [24]. Importantly, key changes in muscle composition, particularly those related to muscle structure and function, were not explored, leaving gaps in understanding the full extent of muscle recovery. Overcoming these limitations, this study confirms that MEST restores total quadriceps volume as well as structural and functional properties in OA models, as demonstrated by MRI, electrophysiological, and immunohistochemical assessments 5 weeks posttreatment.

The restoration of quadriceps volume observed in Fig. 2 suggests that muscle recovery occurs throughout the entire quadriceps. The recovery of quadriceps volume in areas containing the MEST filaments appears to result from muscle fiber regeneration. Mechanical injury from MEST induces a mild, temporary inflammatory response that activates macrophages and muscle stem cells (satellite cells), promoting muscle growth [24]. Macrophages [26,27] and satellite cells [28,29] play critical roles in muscle regeneration following injury. The presence of small muscle fibers around the MEST insertion site (Fig. 7) suggests regeneration, with these new fibers forming and maturing over time. Additionally, a decrease in muscle cell density within the ROI (Fig. 4A-C), suggesting increased individual muscle fiber thickness [21], indicates that MEST contributes to the repair and strengthening of atrophied fibers. Notably, MEST's effects may extend beyond the localized regeneration of muscle fibers around the filaments. The treatment may also promote overall quadriceps hypertrophy, potentially driven by increased activity enabled through pain relief [21]. While fibrosis, marked by excessive extracellular matrix accumulation (especially collagen), may contribute somewhat to muscle volume increase post-injury, it is unlikely to be the primary driver here. Fibrosis generally leads to fibrous scar tissue formation, which replaces functional muscle and can hinder regeneration [30,31]. Thus, an increase in muscle volume due solely to non-functional connective tissues such as scar or fat would contradict the findings of both this study (Fig. 3) and prior research [24], which showed improvements in muscle regeneration and contraction force.

The recovery of maximal hindlimb torque generated by quadriceps contraction (Fig. 3) demonstrates that MEST induces muscle recovery beyond just increases in volume (Fig. 2), weight, or fiber thickness [21,24], thereby enhancing the muscle's overall functional capacity. Data from Fig. 3, collected 5 weeks after MEST treatment, together with previously observed early-stage recovery patterns (showing no improvement at 1 week but recovery at 3 weeks post-treatment to levels similar to those seen in this study) [24], indicate a potential timeframe for peak recovery in muscle contraction, possibly followed by sustained benefits. A clinical trial supports these findings, showing a significant increase in maximum isometric force in the affected leg of OA patients after 4 weeks of MEST treatment [23], with similar benefits observed at 8 weeks post-MEST treatment in another, larger-scale clinical trial (unpublished data). The restored contractile abil-



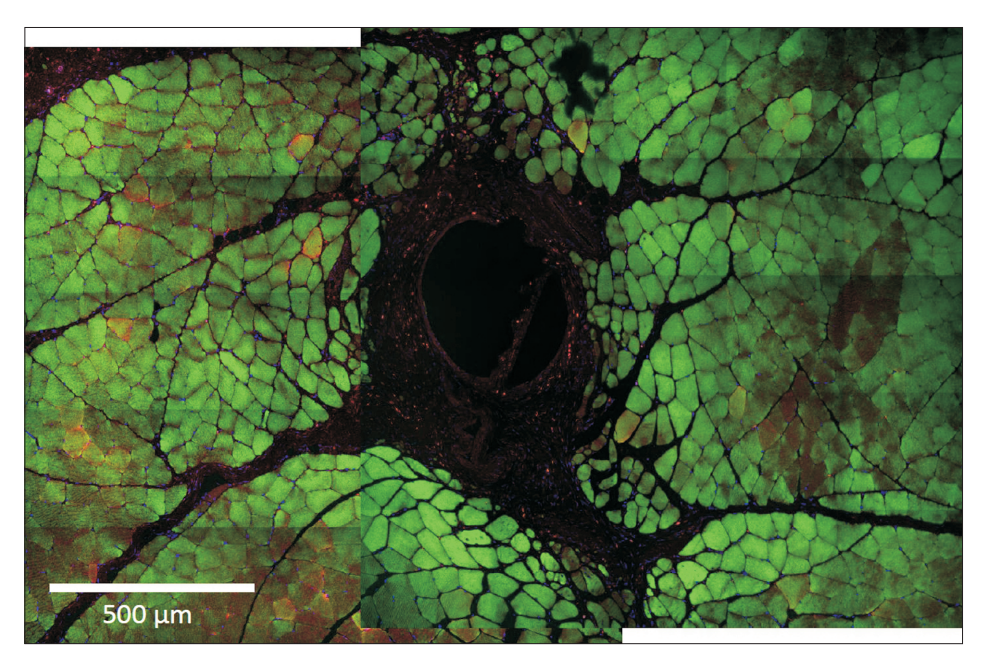


**Fig. 7.** Representative tile scans of immunohistochemically stained quadriceps around the hole generated by the MEST filament in the MIA + MEST group at 5 weeks after treatment. Scale bar =  $500 \mu m$ . Staining: Blue = DAPI; Red =  $\alpha$ -actin; Green = myosin. MEST: Muscle Enhancement and Support Therapy, MIA: monoiodoacetate.

ity of the quadriceps, a fundamental function of skeletal muscle, demonstrates a marked improvement in muscle quality and condition after MEST treatment. Although increases in muscle volume and mass are generally linked to improvements in muscle force and functional strength, factors such as the amount of non-functional muscle components, neuromuscular activation, and the proportion of type II fibers—which produce greater force than type I fibers—may affect functional recovery [32–34]. While further studies are needed to clarify how or even whether MEST influences these factors, MEST may trigger a more natural muscle repair process [24] and encourage physical activity [21], similar to the injury and over-recovery responses seen in exercise-induced muscle hypertrophy [35], rather than targeting specific pathways.

Beyond measures of volume and strength, examining biomarker expression in the quadriceps (**Fig. 4**) offers deeper insight into muscle recovery at a molecular level following MEST treatment.  $\alpha$ -actin and myosin, two essential muscle proteins, are central to skeletal muscle structure and function as they form the scaffold required for stability, contraction, and force generation [36,37].  $\alpha$ -actin, a primary component of the thin filament in the sarcomere, offers structural support and stability by anchoring other proteins, ensuring sarcomere alignment, and allowing it to withstand tension during contraction and relaxation [38]. Increased levels of  $\alpha$ -actin strengthen

the contractile apparatus by providing more binding sites for myosin, enhancing muscle integrity and function. Myosin, the main motor protein in muscle cells, forms thick filaments that interact with  $\alpha$ -actin to generate force through contraction [38]. This force-generating interaction [39] not only facilitates movement but also preserves muscle fiber stability under stress. Thus, the observed recovery of  $\alpha$ -actin and myosin levels (**Fig. 4D, F**) after MEST treatment likely contributes to the restoration of muscle volume, structure, and strength. Additionally, as ATP, the primary energy currency, is essential for muscle contraction and relaxation cycles, particularly the interaction between actin and myosin [39], the increased COX4 levels (Fig. 4H, I), a marker of mitochondrial function [40], likely indicate enhanced mitochondrial biogenesis or activity. These adaptations may represent an effort to enhance overall energy output and improve the muscle's oxidative capacity [41], potentially linked to increased physical activity made possible by MEST's pain-relieving effects [21].

Despite the availability of various treatment options, pain management in OA remains suboptimal for many patients, reflecting a significant unmet clinical need [4]. Current therapies, which largely focus on addressing joint pathology, have limitations that highlight the promise of MEST, a novel approach that targets the weakened quadriceps muscles often associated with knee OA. The ob-



served reversal of both decreased PWT and WBR in MIAtreated OA animals at 5 weeks post-MEST treatment (Fig. 5) provides compelling evidence of the pain-relieving effects of MEST in knee OA. These results are consistent with previous studies [21,22,24], which demonstrated MEST's ability to reduce knee OA pain across different time points, ranging from 1 to 5 weeks post-treatment, by improving mechanical pain sensitivity, limb loading balance, exploratory activity, and rotarod performance. Moreover, MEST treatment has been shown to reduce sensitization of nociceptors innervating the OA-affected knee joint [22]. These findings are further supported by a randomized, blinded clinical trial, which reported significant reductions in weight-bearing pain at 4, 8, 20, and 30 weeks following MEST treatment in patients with Kellgren and Lawrence grade 2 or 3 knee OA [23]. Therefore, MEST demonstrates long-term efficacy as a standalone treatment and, with its distinct mechanism of action, holds potential for integration with existing therapies, offering a more holistic approach to OA pain management.

An important outcome of this study is the observed strong correlation between knee OA pain and quadriceps volume, hindlimb torque force, and biomarker levels (r > 0.4, P < 0.001 for all; **Fig. 6**). This result reinforces the association between muscle health and the pain relief achieved with MEST treatment. Prior research has documented connections between quadriceps weakness and OA progression [6–8], as well as the role of strengthening exercises in pain reduction [42,43]. The findings of the current study extend this knowledge by offering statistical evidence for a more specific link between these individual muscle-related factors and OA pain. Overall, the connection between MEST-induced pain relief and increased muscle volume, contraction force, and biomarker levels highlights the wide-ranging benefits of MEST treatment.

Mechanical loading is known to play a significant role in the progression of OA [44,45]. For this reason, increased quadriceps strength and structural volume are essential in providing joint stability, improving joint mechanics, and reducing mechanical stress on the OA-affected knee [12–18, 20,46,47]. These improvements by MEST together may help reduce pain and support overall joint function.

While this study primarily focused on pain relief through muscle recovery facilitated by PDO filaments, the benefits of MEST may extend beyond the period of filament degradation and the time required for full muscle regeneration. Pain relief from MEST may occur earlier [21] than complete quadriceps recovery which takes several weeks [24]. By stabilizing surrounding muscle tissue and

reducing joint compression forces [23], a particularly valuable effect in humans, where the knee experiences high compressive forces due to bipedal weight-bearing, MEST may improve pain and knee function early in the recovery process. This stabilizing support could promote knee stability and alleviate pain even before muscle regeneration is fully achieved. Moreover, while PDO filaments typically degrade within months [48], the therapeutic effects of MEST, such as pain relief and muscle recovery, may persist well beyond this period. By potentially interrupting the vicious cycle of pain, limited movement, and muscle weakness, MEST may support a positive feedback loop associated with lasting pain relief, increased activity, and muscle recovery. Thus, MEST's ability to promote muscle regeneration and stabilize surrounding muscle tissue together helps maintain knee stability and function, contributing to OA pain relief with both an immediate and long-term impact.

Taken together, this study suggests the promising therapeutic potential of MEST for alleviating knee OA pain by effectively restoring weakened and atrophied quadriceps. This restoration increases overall muscle volume and strength, addressing essential aspects of muscle health while enhancing key biomarkers related to muscle structure, function, and energy metabolism. Each of these factors may contribute to alleviating pain, as demonstrated by their strong correlation with pain relief. However, while significant correlations were observed between quadriceps recovery and pain relief, these findings do not establish a causal relationship. Further mechanistic studies are necessary to confirm whether MEST-induced muscle recovery directly mediates pain relief.

MEST's unique focus on skeletal muscle recovery may offer an encouraging standalone option for OA pain relief, with potential to work synergistically alongside existing treatments. While these results provide a solid foundation, further research is essential to refine treatment protocols for human application, considering anatomical differences. Long-term studies will also be critical to assess the durability of MEST's effects and to identify any potential long-term side effects. Additionally, comparative studies are needed to evaluate MEST's effectiveness in promoting muscle recovery and reducing pain relative to traditional muscle-strengthening therapies. Given its potential, MEST also warrants investigation for treating muscle-wasting diseases across various etiologies.



# **DATA AVAILABILITY**

The data that supporting the findings of this study are available in the results. For further inquiries, please contact the corresponding author.

# **ACKNOWLEDGMENTS**

OV MEDI Co., Ltd provided MEST.

# **CONFLICT OF INTEREST**

JHJ was a full-time employee of OV MEDI Co., Ltd. at the time of manuscript submission. The company did not influence the study design, conduct, or interpretation. The other authors declare no conflicts of interest.

#### **FUNDING**

This study was supported by the Basic Research Program of the National Research Foundation (NRF) funded by the Ministry of Science and ICT (NRF2020R1A2C3008481 and RS-2023-00238538). Additional support was provided by the Soonchunhyang University Research Fund.

#### **AUTHOR CONTRIBUTIONS**

Myeounghoon Cha: Conceptualization, investigation, analysis, and writing – original draft preparation; Guanghai Nan: Investigation and analysis; Nari Kang: Investigation and analysis; Sun Joon Bai: Validation; Ryo Ikeda: Validation; Bae Hwan Lee: Funding acquisition, supervision, and writing – review & editing; Jun Ho Jang: Conceptualization, supervision, and writing – original draft preparation, and writing – review & editing.

#### **ORCID**

Myeounghoon Cha, https://orcid.org/0000-0002-7993-672X Guanghai Nan, https://orcid.org/0000-0001-8238-6899 Nari Kang, https://orcid.org/0009-0005-6199-0604 Sun Joon Bai, https://orcid.org/0000-0001-5027-3232 Ryo Ikeda, https://orcid.org/0000-0001-6603-7146 Bae Hwan Lee, https://orcid.org/0000-0003-4719-9021 Jun Ho Jang, https://orcid.org/0000-0003-3117-1286

#### REFERENCES

- 1. Martel-Pelletier J, Barr AJ, Cicuttini FM, Conaghan PG, Cooper C, Goldring MB, et al. Osteoarthritis. Nat Rev Dis Primers 2016; 2: 16072.
- 2. Hunter DJ, Bierma-Zeinstra S. Osteoarthritis. Lancet 2019; 393: 1745-59.
- 3. Fu K, Robbins SR, McDougall JJ. Osteoarthritis: the genesis of pain. Rheumatology (Oxford) 2018; 57(suppl\_4): iv43-50.
- 4. Block JA, Cherny D. Management of knee osteoarthritis: what internists need to know. Med Clin North Am 2021: 105: 367-85.
- 5. Ghai B, Kumar M, Makkar JK, Goni V. Comparison of ultrasound guided pulsed radiofrequency of genicular nerve with local anesthetic and steroid block for management of osteoarthritis knee pain. Korean J Pain 2022; 35: 183-90.
- 6. Øiestad BE, Juhl CB, Culvenor AG, Berg B, Thorlund JB. Knee extensor muscle weakness is a risk factor for the development of knee osteoarthritis: an updated systematic review and meta-analysis including 46 819 men and women. Br J Sports Med 2022; 56: 349-55.
- 7. Dell'isola A, Wirth W, Steultjens M, Eckstein F, Culvenor AG. Knee extensor muscle weakness and radiographic knee osteoarthritis progression. Acta Orthop 2018; 89: 406-11.
- 8. Segal NA, Glass NA. Is quadriceps muscle weakness a risk factor for incident or progressive knee osteoarthritis? Phys Sportsmed 2011; 39: 44-50.
- 9. Ikemoto-Uezumi M, Matsui Y, Hasegawa M, Fujita R, Kanayama Y, Uezumi A, et al. Disuse atrophy accompanied by intramuscular ectopic adipogenesis in vastus medialis muscle of advanced osteoarthritis patients. Am J Pathol 2017; 187: 2674-85.
- 10. Rice DA, McNair PJ, Lewis GN. Mechanisms of quadriceps muscle weakness in knee joint osteoarthritis: the effects of prolonged vibration on torque and muscle activation in osteoarthritic and healthy control subjects. Arthritis Res Ther 2011; 13: R151.
- 11. Luc-Harkey BA, Safran-Norton CE, Mandl LA, Katz JN, Losina E. Associations among knee muscle strength, structural damage, and pain and mobility in individuals with osteoarthritis and symptomatic meniscal tear. BMC Musculoskelet Disord 2018; 19: 258.
- 12. An KN. Muscle force and its role in joint dynamic stability. Clin Orthop Relat Res 2002; 403 Suppl: S37-42.



- 13. Sarvazyan A, Rudenko O, Aglyamov S, Emelianov S. Muscle as a molecular machine for protecting joints and bones by absorbing mechanical impacts. Med Hypotheses 2014; 83: 6-10.
- 14. Ferenczi MA, Bershitsky SY, Koubassova NA, Kopylova GV, Fernandez M, Narayanan T, et al. Why muscle is an efficient shock absorber. PLoS One 2014; 9: e85739.
- 15. Bennell KL, Hunt MA, Wrigley TV, Lim BW, Hinman RS. Role of muscle in the genesis and management of knee osteoarthritis. Rheum Dis Clin North Am 2008; 34: 731-54.
- 16. Hurley MV. The role of muscle weakness in the pathogenesis of osteoarthritis. Rheum Dis Clin North Am 1999; 25: 283-98, vi.
- 17. Mikesky AE, Meyer A, Thompson KL. Relationship between quadriceps strength and rate of loading during gait in women. J Orthop Res 2000; 18: 171-5.
- Winby CR, Lloyd DG, Besier TF, Kirk TB. Muscle and external load contribution to knee joint contact loads during normal gait. J Biomech 2009; 42: 2294-300.
- 19. Herzog W, Longino D, Clark A. The role of muscles in joint adaptation and degeneration. Langenbecks Arch Surg 2003; 388: 305-15.
- 20. Tanaka R, Hirohama K, Ozawa J. Can muscle weakness and disability influence the relationship between pain catastrophizing and pain worsening in patients with knee osteoarthritis? A cross-sectional study. Braz J Phys Ther 2019; 23: 266-72.
- 21. Lee K, Gang GG, Kang YG, Jung SS, Park HG, Jang JH. Alleviation of osteoarthritis-induced pain and motor deficits in rats by a novel device for the intramuscular insertion of cog polydioxanone filament. Appl Sci 2021; 11: 10534.
- 22. Cha M, Bak H, Lee BH, Jang JH. Alleviation of peripheral sensitization by quadriceps insertion of cog polydioxanone filaments in knee osteoarthritis rats. Biochem Biophys Res Commun 2024; 698: 149549.
- 23. Kim KC, Lee HJ, Lee KY, Park HG. Clinical study on safety, clinical indicators of polydioxanone sutures inserted into vastus medialis muscle in degenerative knee osteoarthritis. Clin Pain 2021; 20: 105-21.
- 24. Cha M, Bak H, Bai SJ, Lee BH, Jang JH. Quadriceps recovery and pain relief in knee osteoarthritis rats by cog polydioxanone filament insertion. Regen Biomater 2024; 11: rbae077.
- 25. de Sousa Valente J. The pharmacology of pain associated with the monoiodoacetate model of osteoarthritis. Front Pharmacol 2019; 10: 974.

- 26. Wang X, Zhou L. The many roles of macrophages in skeletal muscle injury and repair. Front Cell Dev Biol 2022; 10: 952249.
- 27. Novak ML, Weinheimer-Haus EM, Koh TJ. Macrophage activation and skeletal muscle healing following traumatic injury. J Pathol 2014; 232: 344-55. Erratum in: J Pathol 2014; 233: 319.
- 28. Snijders T, Nederveen JP, McKay BR, Joanisse S, Verdijk LB, van Loon LJ, et al. Satellite cells in human skeletal muscle plasticity. Front Physiol 2015; 6: 283.
- Dumont NA, Bentzinger CF, Sincennes MC, Rudnicki MA. Satellite cells and skeletal muscle regeneration. Compr Physiol 2015; 5: 1027-59.
- Lieber RL, Ward SR. Cellular mechanisms of tissue fibrosis.
  Structural and functional consequences of skeletal muscle fibrosis. Am J Physiol Cell Physiol 2013; 305: C241-52.
- 31. Mahdy MAA. Skeletal muscle fibrosis: an overview. Cell Tissue Res 2019; 375: 575-88.
- 32. Folland JP, Williams AG. The adaptations to strength training: morphological and neurological contributions to increased strength. Sports Med 2007; 37: 145-68.
- 33. Seynnes OR, de Boer M, Narici MV. Early skeletal muscle hypertrophy and architectural changes in response to high-intensity resistance training. J Appl Physiol (1985) 2007; 102: 368-73.
- 34. Häkkinen K, Komi PV. Electromyographic and mechanical characteristics of human skeletal muscle during fatigue under voluntary and reflex conditions. Electroencephalogr Clin Neurophysiol 1983; 55: 436-44.
- 35. Schoenfeld BJ. Does exercise-induced muscle damage play a role in skeletal muscle hypertrophy? J Strength Cond Res 2012; 26: 1441-53.
- 36. Koubassova NA, Tsaturyan AK. Molecular mechanism of actin-myosin motor in muscle. Biochemistry (Mosc) 2011; 76: 1484-506.
- 37. Clark KA, McElhinny AS, Beckerle MC, Gregorio CC. Striated muscle cytoarchitecture: an intricate web of form and function. Annu Rev Cell Dev Biol 2002; 18: 637-706.
- 38. Henderson CA, Gomez CG, Novak SM, Mi-Mi L, Gregorio CC. Overview of the muscle cytoskeleton. Compr Physiol 2017; 7: 891-944.
- 39. Squire J. Special issue: the actin-myosin interaction in muscle: background and overview. Int J Mol Sci 2019; 20: 5715.
- 40. Li Y, Park JS, Deng JH, Bai Y. Cytochrome c oxidase



- subunit IV is essential for assembly and respiratory function of the enzyme complex. J Bioenerg Biomembr 2006; 38: 283-91.
- 41. Dong H, Tsai SY. Mitochondrial properties in skeletal muscle fiber. Cells 2023; 12: 2183.
- 42. Anwer S, Alghadir A. Effect of isometric quadriceps exercise on muscle strength, pain, and function in patients with knee osteoarthritis: a randomized controlled study. J Phys Ther Sci 2014; 26: 745-8.
- 43. Imoto AM, Peccin MS, Trevisani VF. Quadriceps strengthening exercises are effective in improving pain, function and quality of life in patients with osteoarthritis of the knee. Acta Ortop Bras 2012; 20: 174-9.
- 44. Vincent KR, Conrad BP, Fregly BJ, Vincent HK. The pathophysiology of osteoarthritis: a mechanical perspective on the knee joint. PM R 2012; 4(5 Suppl):

- S3-9.
- 45. Shaktivesh, Malekipour F, Lee PVS. Shock absorbing ability in healthy and damaged cartilage-bone under high-rate compression. J Mech Behav Biomed Mater 2019; 90: 388-94.
- 46. Rudenko OV, Tsyuryupa S, Sarvazyan A. Skeletal muscle contraction in protecting joints and bones by absorbing mechanical impacts. Acoust Phys 2016; 62: 615-25.
- 47. Murray AM, Thomas AC, Armstrong CW, Pietrosimone BG, Tevald MA. The associations between quadriceps muscle strength, power, and knee joint mechanics in knee osteoarthritis: a cross-sectional study. Clin Biomech (Bristol) 2015; 30: 1140-5.
- 48. Hochberg J, Meyer KM, Marion MD. Suture choice and other methods of skin closure. Surg Clin North Am 2009; 89: 627-41.